Title
NUCLEAR RADII FROM ALPHA-PARTICLE SCATTERING AND ALPHA-RADIOACTIVITY

Author
Rasmussen, John O.

Publication Date
1958

UCRL 8124

UNIVERSITY OF CALIFORNIA

Radiation Laboratory

BERKELEY, CALIFORNIA

UCRL-8124

UNIVERSITY OF CALIFORNIA
Radiation Laboratory
Berkeley, California

Contract No. W-7405-eng-48

NUCLEAR RADII FROM ALPHA-PARTICLE SCATTERING AND ALPHA-RADIOACTIVITY

John O. Rasmussen

January 1958

Printed for the U. S. Atomic Energy Commission

NUCLEAR RADII FROM ALPHA-PARTICLE SCATTERING AND ALPHA-RADIOACTIVITY

John O. Rasmussen

Radiation Laboratory and Department of Chemistry
University of California, Berkeley, California

January, 1958

Introduction

While we are here collecting our ideas about nuclear sizes, I am reminded of the Birmingham Nuclear Physics Conference of four years ago. One of the high points of that conference was the talk of Professor Hofstadter, who described the electron scattering experiments which established nuclear charge distributions smaller than the size values generally accepted then. One question raised was: "How can these radii be consistent with the larger radii inferred from alpha decay data?" This is one of the central questions I wish to discuss here, and to help us there have come, in the short span of time since Birmingham many important measurements from inelastic and elastic cross sections for alpha particle bombardments on complex nuclei.

In the space of a few years we have reached a more sophisticated level in our concepts of nuclear size. We divide experimental measurements of size into two categories; first, those measuring the charge (or matter) density distribution, such as electron scattering, and, second, those measuring the form of some nuclear potential, such as measurements of nucleon or alpha particle interactions with nuclei. The second type of measurements quite generally yield larger measures of size than do the first. Another degree of sophistication comes from considering the diffuse nature and occasionally the non-sphericity of the nuclear surface, both as regards matter distributions and the various nuclear potentials.

Radius Determinations with Sharp Cut-off Models

Many interpretations of the measurements of size of the nuclear potential for alpha particles are based on "sharp-cut-off" models which ignore any diffuseness of the potential and yield an effective nuclear radius parameter, R. We wish to survey results from such interpretations first. Some types of measurements which we now wish to compare have not been made over wide enough range of mass number A to establish the two parameters in the formula $R = a A^{1/3} + b$. We shall therefore compare the R values at the mass number 209. This mass number lies near the lower border of the principal region of alpha emitters and near the upper border of the heavy stable nuclei usable as targets in alpha bombardment experiments. Furthermore, the nucleus Bi^{209} is surely spherical, lying adjacent to doubly-magic Pb^{208}.

Alpha decay rate data for even-even nuclei may be interpreted in terms of sharp cut-off coulombic barrier penetration theory, and we are provided with a set of R values for various alpha emitters.[1] Unfortunately for the applicability of alpha decay rates to measuring nuclear size, there is uncertainty about the fundamental rate of formation of alpha particles by nuclei; that is, we are uncertain regarding the hypothetical "decay rate in the absence of the barrier," f, or reduced width for alpha emission, δ^2 (=hF). Various alpha decay models have been proposed with f ranging from $\sim 10^{21}$ sec^{-1} in the one-body models to $\sim 10^{15}$ sec^{-1} in the form of many-body model proposed by Bethe[2] in 1937. Various other models have led to predictions intermediate between these extremes. Table I shows the R values (in units of fermis, 10^{-13} cm) indicated for A = 209 by an analysis of even-even alpha emitters with more than 126 neutrons, using the two extreme models mentioned.

The measurement of cross sections for nuclear inelastic processes in alpha particle bombardment of nuclei affords another source of radius values, R.

Uranium and other available heavy element targets have been used in radiochemical studies of total (fission plus spallation) reaction cross sections as a function of alpha energy. Fig. 1 shows one such excitation function[3] compared to theoretical values[4] for two different assumed radii. The results of such studies would extrapolate to a value of R of 10.4 for mass 209. (Distances given in this paper are understood to be in units of 10^{-13} cm.)

A few years ago the total inelastic cross sections of carbon, copper, and tantalum for 240 Mev alpha particles were measured by a beam attenuation technique.[5] The resulting radius formula derived from these measurements gives, when extrapolated to mass 209, an R value of 11.3.

For several light nuclei ($A \lesssim 30$) measurements of angular distributions of inelastically scattered alpha particle groups have been made.[6] In many cases these angular distributions show diffraction maxima and minima much like those observed in deuteron stripping. By fitting the distributions to the theoretical expressions of Austern, Butler, and McManus[7] an effective nuclear interaction radius is obtained. Of course, it is a long extrapolation from these nuclei to mass 209, but we include in Table I an approximate extrapolated radius figure of ~10.8.

Our most extensive knowledge of the nuclear radius for alpha particles and its variation with mass number comes from alpha elastic scattering cross section measurements. Fig. 2, taken from a paper by Igo and Thaler,[8] shows the angular variation of elastic cross sections for 40.2 Mev alpha particles, plotted as the ratio to the point charge coulomb scattering cross section. One sees diffraction structure in the lighter nuclei, but for Ta and heavier nuclei the fall-off with angle is generally smooth, though a semblance of diffraction structure is evident at Pb.[9] Other interesting features may be seen by examination of the variation of cross section with energy at fixed angles. Fig. 3, from the work of Kerlee, Blair, and Farwell, shows such a plot.[10] One notes a

Table I

Sharp Cut-off Radii from Various Measurements

General type	Particular model or experiment	Indicated radius at mass 209 (10^{-13} cm)	References
I. Alpha decay	One body model $f \sim 10^{21}$ sec^{-1}	9.3	1, 2
	Extreme many-body model $f \sim 10^{15}$ sec^{-1}	12.2	2
II. Alpha cross sections for inelastic processes	a. Reaction cross sections (fission + spallation) in heavy elements near threshold	10.4	3
	b. 240 Mev alpha reaction cross sections	11.3	5
	c. (α,α') angular distributions in light elements	~10.8 (extrap.)	6
III. Alpha elastic scattering	Sharp cut-off model	10.6	10

significant rise above the coulomb cross section before the drop in the case of Pb^{208} and Bi^{209}. The rise is less pronounced in Pb^{207} and Pb^{206} and is absent for several target elements not shown in Fig. 3. The studies of Kerlee et al.[10] cover a wide range of elements and energies and are analyzed by a sharp cut-off model[11] in which a pure coulombic barrier is assumed beyond a cut-off radius, R, defining a surface which is totally absorbing. That is, the nucleus is assumed to be completely black to partial waves with angular momentum less than critical, and partial waves with $\ell \geq \ell_c$ are assumed to give their full coulomb scattering contribution. This model fails to reproduce the data at large angles but gives reasonable fits at small angles. Fig. 4 is from the paper of Kerlee et al.[10] and shows a plot of R values deduced with this model. The radii are best fitted by the formula $R = 1.414\ A^{1/3} + 2.190$. Significant deviations away from the best fit are to be seen, and considerable short-term variations are sometimes to be seen among nearly neighboring nuclei.

Size Interpretations with Diffuse Potentials

Optical model analyses have given excellent fits of alpha elastic scattering angular distributions. These analyses have generally used a form factor for real and imaginary potential of the familiar Woods-Saxon type,[12]

$$\frac{V + i\,W}{1 + \exp\left(\frac{r - r_o}{d}\right)} .$$

The parameter d measures the diffuseness, and r_o is the radius at which the nuclear potential has fallen to half its central value. Igo and Thaler[8] have published the following parameters as best fitting 40 Mev alpha scattering data:

$$r_o = 1.35\ A^{1/3} + 1.3,\ d = 0.5,\ V = -45\ \text{Mev},\ W = -10\ \text{Mev}.$$

These potentials signify a short mean free path (~2 fermis) for the alphas in nuclear matter. There now seems to be some question as to how unique these values of the parameters are. Cheston and Glassgold[13] find good fits are obtainable with widely different values of V if the r_o value is simultaneously adjusted; i.e., the effect of deepening the potential V can be compensated by decreasing r_o.[14] It is of considerable interest that the depth of the real potential is less for 22 Mev alphas than for 40 Mev,[8] the reverse of the behavior of the real potential for neutron or proton scattering.

We may make some comparison between the optical model potential and the nuclear charge distribution, since both have been analyzed using the same form factor. At mass 209 we would find that the Igo-Thaler potential falls to half its central value at a distance at 9.3 and to one-tenth (i.e. 4.5 + i 1.0 Mev) at 10.4. The real potential would have fallen to 1 Mev at 11.2.

Electron scattering analysis[15] on bismuth indicates that the nuclear charge density falls to half its central value at 6.47 and to one-tenth at 7.82. It is of interest to note that electron scattering in helium by McAllister and Hofstadter[16] showed the alpha particle to be diffuse with an r.m.s. radius of 1.6. This finite size of the alpha particle probably contributes to the extension of the alpha-nuclear potential beyond the matter distribution, but the finite range of nuclear forces and other details probably also contribute to the extension.

Can we now apply the concept of diffuseness of the potential toward understanding the various sharp cut-off radii discussed earlier and summarized in Table I?

Blair[17] has rather thoroughly analyzed the connection of his sharp cut-off radii deduced from alpha elastic scattering to the optical model potentials. Simply stated, the pure coulombic barrier at the sharp cut-off radius and the diffuse optical model potential giving the best fit to a given set of scattering data usually have in common the same critical ℓ_c value for the partial wave that can just surmount the coulombic plus centrifugal barrier. From this connection it is apparent that the indicated sharp cut-off radius will be just slightly larger (because of the diffuse tail) than the radius at the maximum of the optical model barrier. At the sharp cut-off radius of 10.66 in Table I the optical model potential has fallen to around 3 Mev.

The fission-spallation reaction determination gives the value of R = 10.4, closely similar to the alpha elastic value for reasons similar to those above. The "black" nucleus will almost totally absorb partial waves which can surmount the barrier, and these absorbed waves make up the total reaction cross section. Again the analysis will yield a sharp cut-off radius which gives equivalent values of critical angular momentum to those given by the true diffuse potential in the energy range considered.

The 240-Mev alpha inelastic processes, study of which indicates the large radius R = 11.3, must be especially sensitive to the tail of the nuclear potential. Since the optical model potential is energy-dependent and is probably even stronger at this high energy than at 40 Mev, we are not justified in detailed comparison with the optical model potentials for 40 or 22 Mev alphas.

The alpha-inelastic scattering angular distributions in the light elements indicate an effective interaction distance just somewhat larger than the alpha-elastic sharp cut-off radii. The values seem plausible, but we shall not attempt any detailed comparative analysis here.

How will the introduction of a diffuse nuclear potential affect the interpretation of alpha decay rate data? As a first step in answering this question, I have programmed and carried out computations on an IBM-650 computer giving barrier penetration factors (WKB approximation) for all even-even alpha emitters based on the Igo-Thaler optical model potential derived from the extensively analyzed 40 Mev alpha scattering. (Optical model analysis of scattering at energies more comparable to alpha decay energies would be useful in giving a more appropriate potential.) Using alpha decay half lives and the diffuse-potential barrier penetrabilities, the reduced widths[18] for alpha emission, δ^2, are derived in each case. (δ^2 is Planck's constant h times the "frequency factor" f). The lower half if Fig. 5 shows a plot of these reduced widths versus neutron number, and the upper half gives corresponding values for a sharp cut-off radius of 9.3 fermis for all even-even alpha emitters. In the upper plot one sees (for $N > 126$) reduced widths averaging about one Mev as given theoretically by the Preston form[19] of the one body model; this agreement, of course, is the criterion for selection of 9.3 as radius in the first place.

The reduced widths from the diffuse potential show similar trends, but the magnitudes (for $N > 126$) average about a factor of five lower than the one-body values. The break at 126 neutrons is less for the diffuse potential. The diffuse potential gives reasonable values of reduced widths, within the large (factor of 10^6) uncertainty in the theoretical values. Perhaps such applications of optical model potentials can stimulate further developments in fundamental alpha decay theory. Already we can say from these exploratory calculations that reduced widths predicted by the one body model are much closer to the truth than are those of most many body models.

Consequences of Non-Spherical Nuclear Shapes and of Zero-Point Surface Oscillations

There are other details besides the intrinsic diffuseness of the nuclear surface which should eventually be taken into account in the interpretation of the various size-measuring experiments we have discussed. First, there is abundant evidence that the large class of nuclei distant from closed shells take on stabilized spheroidal deformation[20] with eccentricities as high as 0.3. Second, there are surely zero-point oscillations of the nuclear surface.

In first approximation both these effects may be considered as simply giving extra contributions to the apparent diffuseness of the nuclear potential or matter distribution being considered. Some discussion of the special consequences of spheroidal deformation to the alpha-scattering problem is made by Kerlee et al.[10] with reference given to work of Drozdov.[21]

Spheroidal deformation has important special consequences for the detailed interpretation of alpha decay, especially as regards the significance of the relative intensities of decay to various members of a nuclear rotational band system. We have carried inward numerical integrations of the alpha decay wave equation for Cm^{242} up to the spheroidal nuclear surface,[22] fixing the boundary conditions at large distance by use of experimental alpha group intensities to the ground rotational band ($\ell = 0,2,4,6,8$ groups observed). The boundary conditions are not uniquely determined by this procedure, since there are two possible phase choices for each alpha group considered. By indirect arguments based on angular correlation and intensity studies of neighboring odd mass alpha emitters, we believe that the $\ell = 0$, $\ell = 2$, and $\ell = 4$ groups are all in phase within the barrier, although the arguments regarding the $\ell = 4$ phase are not conclusive. Since we are completely uncertain regarding the relative phases of $\ell = 6$ and $\ell = 8$ groups included in our treatment, we are left with four possible solutions. In Fig. 6 are shown plots of the possible alpha wave functions over the spheroidal nuclear surface. Whichever case represents the true physical situation, we see evidence for there being especially preferred zones for alpha emission on the spheroidal surface. Tentative explanations of such non-uniform alpha wave functions have been advanced as follows: Either the alpha maxima represent zones of preferred alpha formation, reflecting zones of greatest probability of finding the most lightly bound nucleons, or the alpha maxima imply higher order surface deformations extending the surface in the regions of the maxima. We may hope from such studies to gain some information on surface deformations of order greater than two.

Regarding information on zero-point surface vibration amplitudes it seems possible that alpha decay can give us some clues. In the Cm^{242} decay scheme shown in Fig. 7 one notes, in addition to decay groups to the ground rotational band, decay to a 1- level, probably to be associated with a first-excited octopole vibrational level, and decay to a high-lying 0+ level, associated with a first excited quadrupole surface vibration of the type preserving cylindrical symmetry (β-vibration).[20] The intensities of alpha decay to these excited vibrational states should be a function of the amplitude of zero-point oscillation. Careful quantitative treatment of the problem has not been completed yet. Qualitatively we may consider a semi-classical argument: Because of the strong dependence of barrier penetrability on barrier thickness, alpha emission will preferentially occur from a surface element during its maximum outward excursions in vibration. This preference will lead to a finite probability that the daughter nucleus is left in a vibrationally excited state following alpha emission.

Conclusion

Our knowledge of the nuclear potential for alpha particles has certainly been greatly enhanced in recent years, principally by alpha elastic scattering studies. Extension of these studies and further careful optical model analysis is important, but the short mean-free path of alpha particles in nuclear matter limits such analysis mainly to exploration of the potential in the nuclear surface region. There seems to be some problem of non-uniqueness of optical model fits. In this situation there is great need for theoretical aid of a fundamental sort, such as estimates in infinite nuclear matter of the real potential and effective mass for alpha particles at various matter densities and for various velocities of travel. There is, as mentioned earlier, some evidence from optical model work that the real attractive potential becomes more attractive with increasing alpha energy, the reverse of the trend[23] for protons or neutrons. We might speculate that this behavior is a result of the special operation of the exclusion principle for complex particles in nuclear matter. The slower the alphas, the lower the effective mass or the less attractive the nuclear potential they would experience, since the Fermi momentum spheres of nucleons in the alpha particle and in the nuclear matter would more seriously overlap for low velocities. It is even possible that alpha particles might find a potential minimum in the surface region where the nuclear density is low yet where they are within range of attractive nuclear forces. Quantitative answers to these speculative questions could go a long way toward fixing a unique choice of optical model potential parameters and furthering the understanding of the fundamentals of alpha decay.

This work was performed under the auspices of the U. S. Atomic Energy Commission.

References

1. cf. I. Perlman and J. O. Rasmussen, "Alpha Radioactivity" Handbuch der Physic, Vol. 42, Springer-Verlag, Berlin (1957).

2. H. A. Bethe, Revs. Modern Phys. 9, 69 (1937).

3. Vandenbosch, Thomas, Vandenbosch, Glass, and Seaborg, Phys. Rev. (to be published).

4. J. M. Blatt and V. F. Weisskopf, "Theoretical Nuclear Physics" Wiley and Sons: New York, (1952) p. 352.

5. Millburn, Birnbaum, Crandall, and Schecter, Phys. Rev. 95, 1268 (1954).

6. See original references in Table II of paper by D. D. Kerlee, J. S. Blair, and G. W. Farwell, Phys. Rev. 107, 1343 (1957).

7. N. Austern, S. T. Butler, and H. McManus, Phys. Rev. 92, 350 (1953).

8. G. Igo and R. M. Thaler, Phys. Rev. 106, 126 (1957).

9. R. E. Ellis and L. Schecter, Phys. Rev. 101, 636 (1956).

10. D. D. Kerlee, J. S. Blair, and G. W. Farwell, Phys. Rev. 107, 1343 (1957).

11. J. S. Blair, Phys. Rev. 95, 1218 (1954).

12. R. D. Woods and D. S. Saxon, Phys. Rev. 95, 577 (1954).

13. W. B. Cheston and A. E. Glassgold, Phys. Rev. 106, 1215 (1957).

14. In the discussion following the present paper and in Dr. Igo's own talk a few days later, he pointed out that studies subsequent to his and Thaler's original publication showed that almost equally good optical model fits could be secured with various combinations of V and r_o that gave the same potential tail at large radius. That is, various combinations that kept V exp (r_o/d) constant gave almost equally good fits, although the best fits were secured with the parameters they originally published as unique.

It indeed seems reasonable that the alpha scattering analysis can only probe the potential in the surface region, since the mean-free path for absorption is so short. An optical model exponential potential in the surface region might be defined by three parameters, instead of the four in the Woods-Saxon expression. The three parameters would be the diffuseness parameter d and magnitude parameters for real and imaginary potential. These three parameters are probably uniquely determinable, but it appears that variation of the diffuseness parameter has not yet been done systematically enough to say that its value is well-determined.

15. B. Hahn, D. G. Ravenhall, and R. Hofstadter, Phys. Rev. 101, 1131 (1957). cf. also K. W. Ford and D. L. Hill, Ann. Rev. Nucl. Sci. 5, 25 (1955).

16. R. W. McAllister and R. Hofstadter, Phys. Rev. 102, 851 (1956).

17. J. S. Blair, Phys. Rev. 108, 827 (1957).

18. R. G. Thomas, Prog. Theo. Phys. 12, 253 (1954). cf. also Ref. 1, p. 149.

19. M. A. Preston, Phys. Rev. 71, 865 (1947).

20. cf. Alder, Bohr, Huus, Mottelson, and Winther, Revs. Modern Phys. 28, 432 (1956).

21. S. I. Drozdov, Soviet Physics 1, 588, 591 (1955) L.

22. cf. J. O. Rasmussen and B. Segall, Phys. Rev. 103, 1298 (1956). J. O. Rasmussen and E. R. Hansen, Phys. Rev. (in press). E. Pennington and M. A. Preston (to be published).

23. cf. A. E. Glassgold and P. J. Kellogg, Phys. Rev. (to be published).

Figure Captions

Fig. 1 A plot from Ref. 3 of total reaction cross section (fission plus spallation) versus energy for alpha particle bombardment of U^{235}. The dashed curves are based on theoretical values of Blatt and Weisskopf[4] for two different choices of radius.

Fig. 2 A plot from Ref. 8 of the experimental ratio of the elastic scattering cross section to the pure Rutherford scattering cross section for 40.2 Mev alpha particles.

Fig. 3 A plot from Ref. 10 of cross section versus energy for elastic scattering of alpha particles from Pb^{206}, Pb^{207}, Pb^{208}, and Bi^{209} at 42° (in the laboratory system).

Fig. 4 A plot from Ref. 10 of the sharp cut-off radii from elastic scattering of alpha particles. The radii are plotted against the cube root of the mass number. The straight line represents a least squares best fit.

Fig. 5 Alpha decay reduced widths, δ^2, for ground state transitions of all even-even alpha emitters are plotted against neutron number (of the parent nucleus). Barrier penetrabilities were calculated in the upper plot by the usual sharp cut-off of a pure coulombic potential, a cut-off radius of 9.3×10^{-13} cm being chosen to give δ^2 values in agreement with one-body theory. Barrier penetrabilities were calculated in the lower plot using a diffuse nuclear potential defined by the Igo-Thaler optical model parameters for 40 Mev alpha particles.[8]

Fig. 6 Alpha wave functions are plotted versus polar angle on the spheroidal nuclear surface of Cm^{242} defined in the work of Rasmussen and Hansen.[22] Boundary conditions for the solutions at large distance are based on experimental relative intensities of alpha decay groups to 0, 2, 4, 6, and 8 spin states in the ground rotational band of the daughter. All cases represent a choice of $\ell = 0$, 2, and 4 waves in phase (+) in the barrier, and the relative phases of $\ell = 6$ and 8 waves are indicated by signs in the upper right-hand corner of each of the four plots.

Fig. 7 Alpha decay scheme of Cm^{242}.

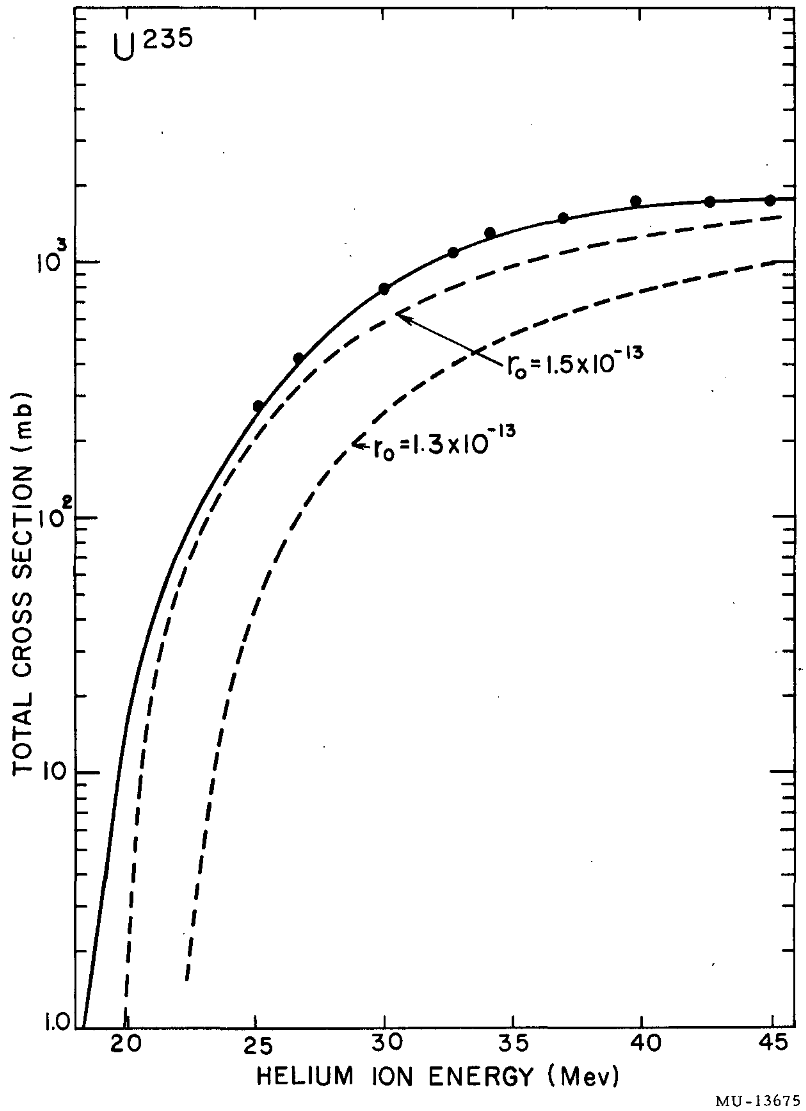
U235
TOTAL CROSS SECTION (mb)
HELIUM ION ENERGY (Mev)
r0 = 1.5x10-13
r0 = 1.3x10-13
1.0
10
10²
10³
20
25
30
35
40
45
MU-13675

Fig. 1.

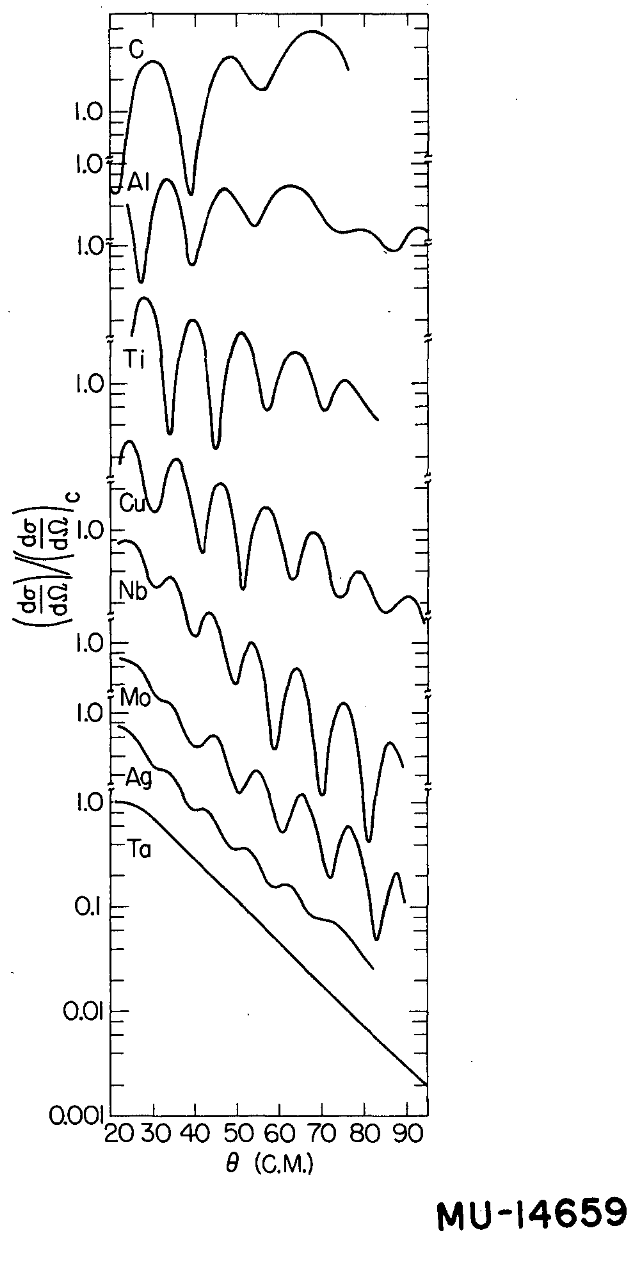
C
Al
Ti
Cu
Nb
Mo
Ag
Ta
1.0
0.1
0.01
0.001
20 30 40 50 60 70 80 90
θ (C.M.)
(dσ/dΩ)/(dσ/dΩ)c
MU-14659

Fig. 2.

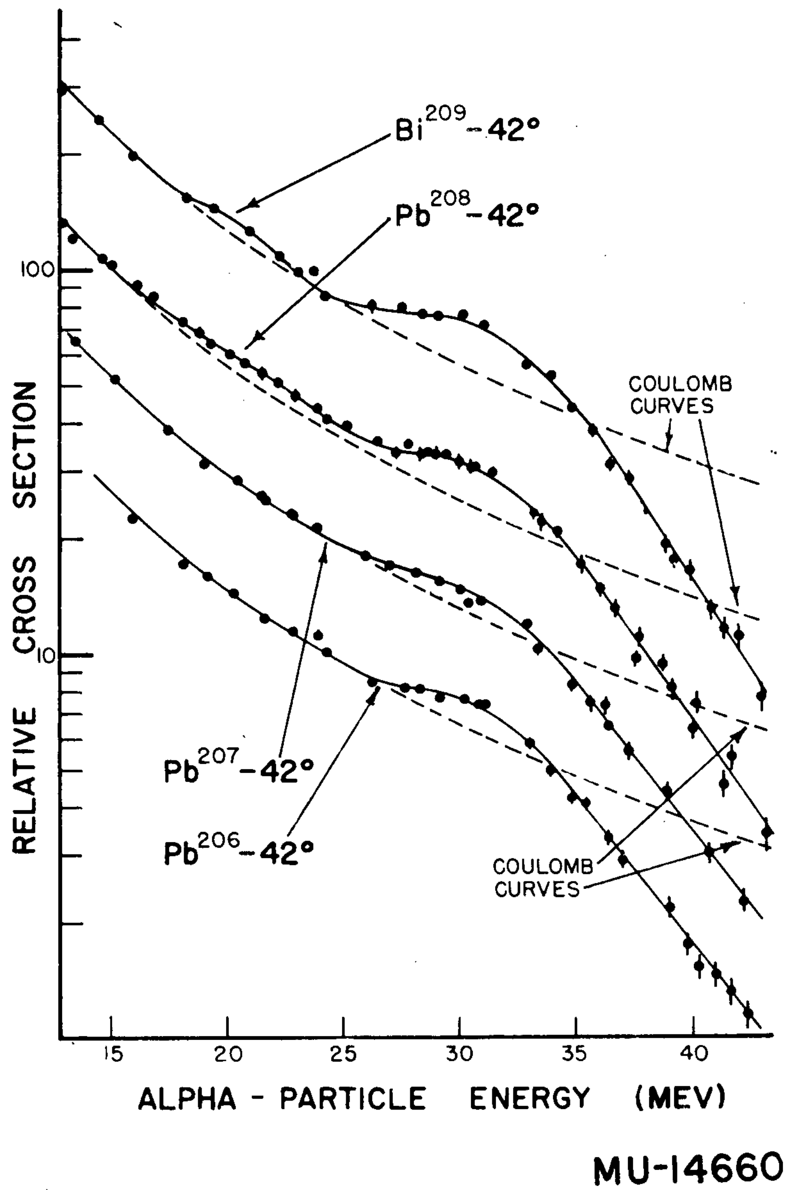
Bi209-42°
Pb208-42°
Pb207-42°
Pb206-42°
COULOMB CURVES
COULOMB CURVES
100
10
RELATIVE CROSS SECTION
15
20
25
30
35
40
ALPHA - PARTICLE ENERGY (MEV)
MU-14660

Fig. 3.

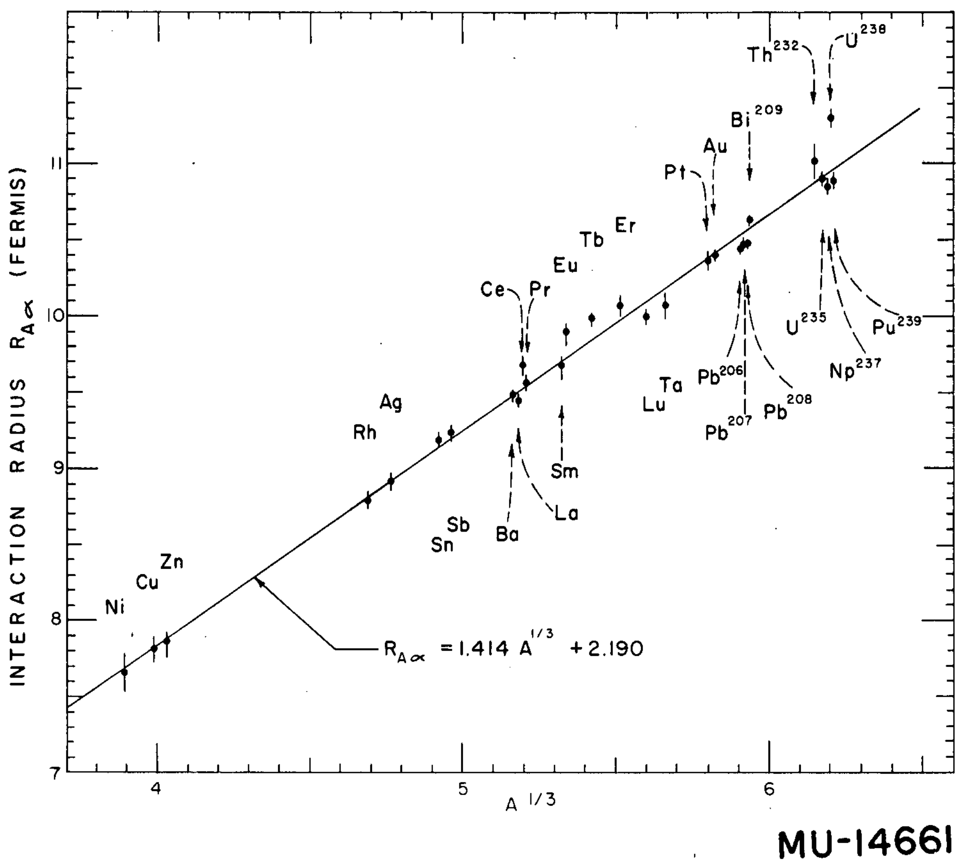
INTERACTION RADIUS $R_{A\alpha}$ (FERMIS)
$A^{1/3}$
$R_{A\alpha} = 1.414\ A^{1/3} + 2.190$
Ni
Cu
Zn
Sn
Sb
Rh
Ag
Ba
La
Ce
Pr
Sm
Eu
Tb
Er
Lu
Ta
Pt
Au
Bi 209
Pb 206
Pb 207
Pb 208
Th 232
U 238
U 235
Np 237
Pu 239
7
8
9
10
11
4
5
6
MU-14661

Fig. 4.

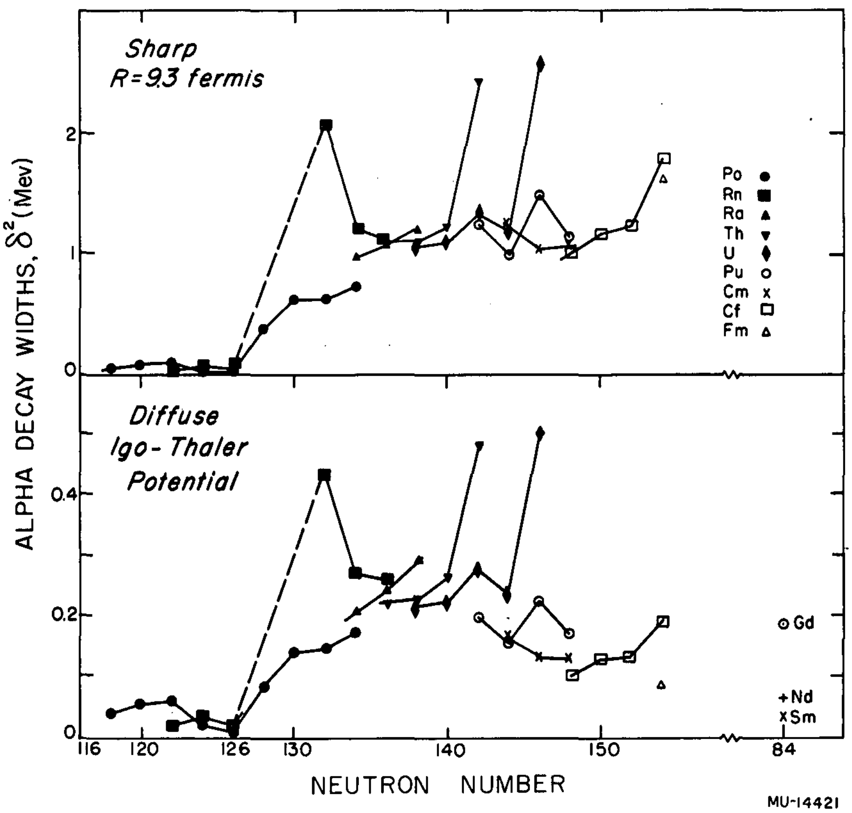
Sharp
R=9.3 fermis
Diffuse
Igo-Thaler
Potential
ALPHA DECAY WIDTHS, δ^2 (Mev)
NEUTRON NUMBER
Po
Rn
Ra
Th
U
Pu
Cm
Cf
Fm
Gd
+Nd
xSm
0
1
2
0.2
0.4
116
120
126
130
140
150
84
MU-14421

Fig. 5.

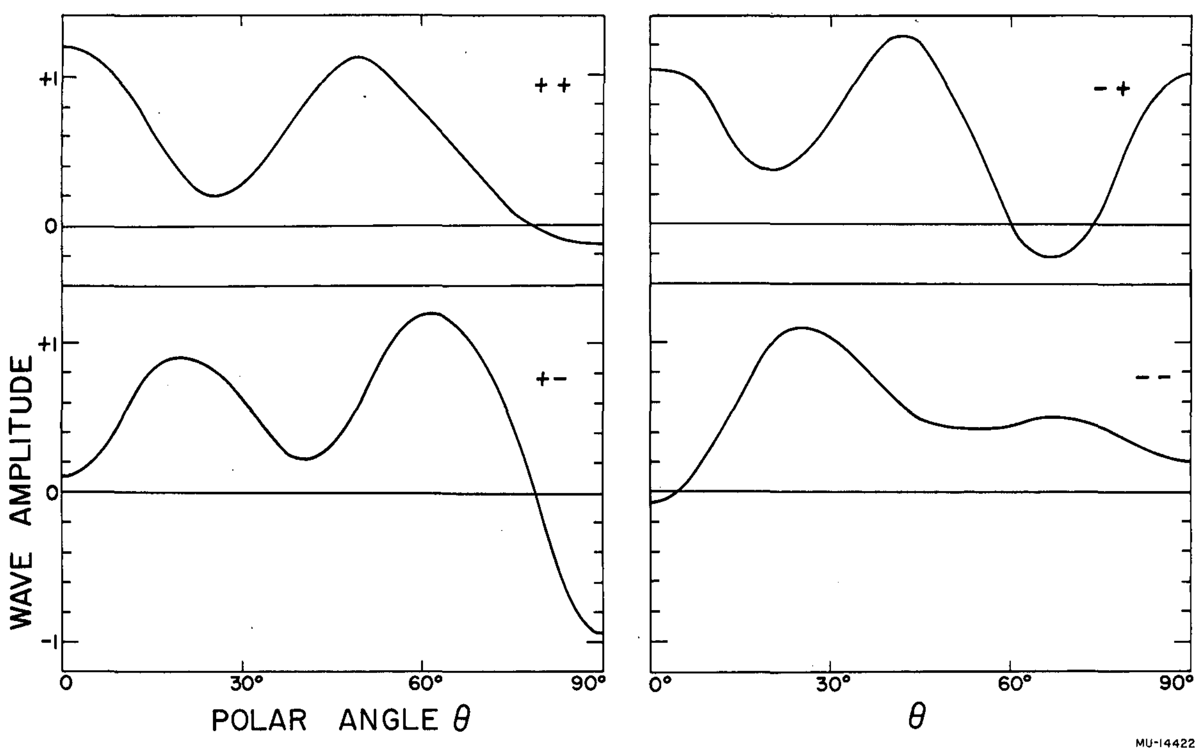

Fig. 6.

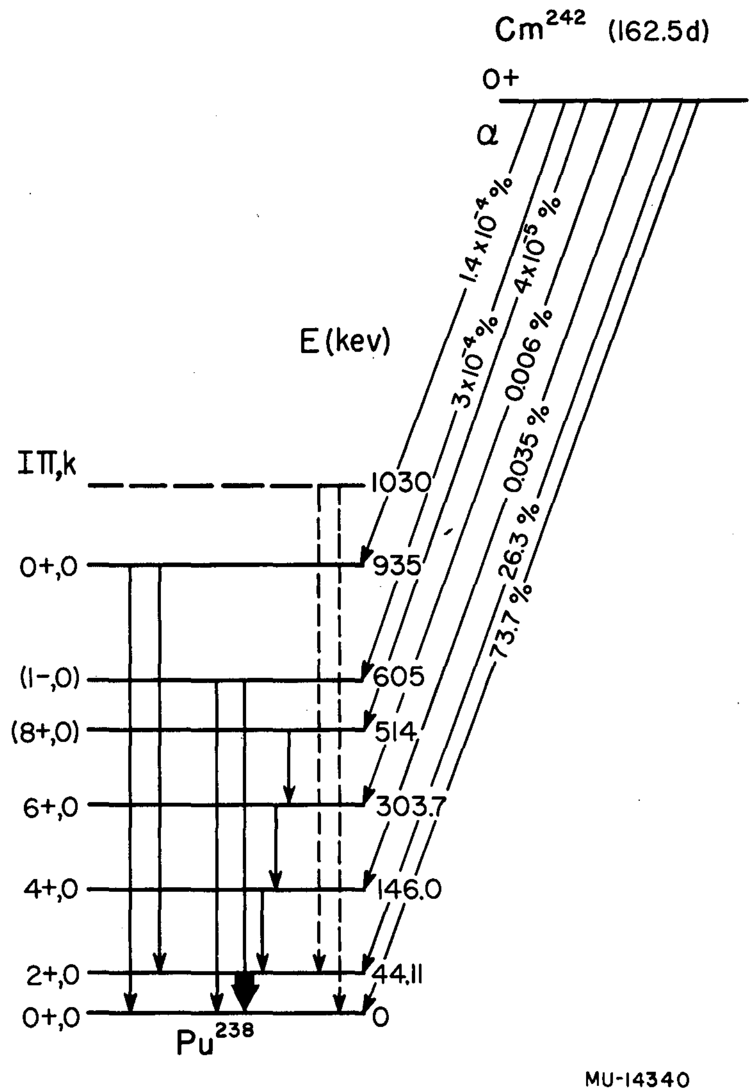
Cm^{242} (162.5d)
0+
α
1.4x10^{-4} %
4x10^{-5} %
3x10^{-4} %
0.006 %
0.035 %
26.3 %
73.7 %
E(kev)
IΠ,k
1030
0+,0
935
(1-,0)
605
(8+,0)
514
6+,0
303.7
4+,0
146.0
2+,0
44.11
0+,0
0
Pu^{238}
MU-14340

Fig. 7.